EPSRC
Engineering and Physical Sciences Research Council

InFoMM
Industrially Focused Mathematical Modelling

EPSRC Centre for Doctoral Training in Industrially Focused Mathematical Modelling

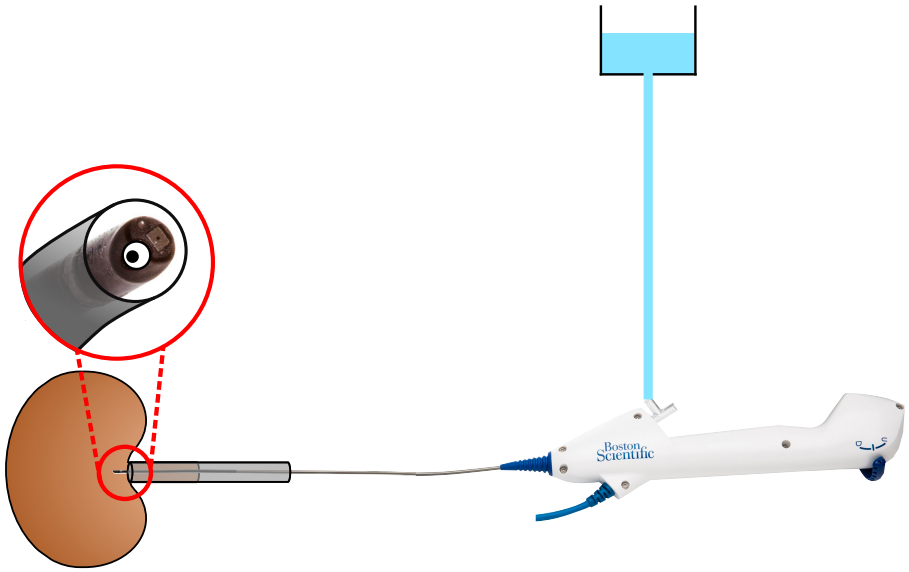

Mathematical modelling of ureteroscopic flows during kidney stone removal

Jessica Williams

UNIVERSITY OF OXFORD

Boston Scientific

Contents

1 Introduction

Background

Ureteroscopy is a minimally invasive surgical procedure for kidney stone removal.

The likelihood of developing kidney stones is on the rise [1], and recent data reports a nine percent lifetime affliction rate in the United States [2]. A common method for stone removal is *flexible uretero-renoscopy*; surgery performed with a hand-held device, a ureteroscope, an endoscope designed to visualise and work within the ureter and kidney (Figure 1). The scope shaft is inserted through the urethra of the anaesthetised patient, passing through the bladder and the ureter, until its tip reaches the *renal pelvis*, the hollow cavity within the kidney where stones commonly form. A light and a minuscule camera embedded within the scope tip transmit a live digital image which enables the urological surgeon to locate stones. Flexible, as opposed to rigid ureteroscopes, have an actively deflectable tip; approximately 6 cm at the distal end of the scope that is steerable through operation of a small lever at the base of the handle (Figure 1). This degree of controllability allows superior access to remote areas of the urinary system [3]. Within the shaft of the scope is a hollow cylindrical channel, the *working channel*. The stone-removal procedure is performed by passing auxiliary instruments, *working tools* (commonly laser fibres or stone baskets), through the working channel to break up and capture stone fragments. Stone destruction in conjunction with ureteroscopy is performed via *laser lithotripsy*; a long, thin fibre optic transmits laser power through the ureteroscope and laser pulses create shock waves to fragment stones. One of two disparate lasering methodologies is typically adopted to facilitate stone removal: stone *dusting*, in which the laser is fired at sufficiently high frequency to obliterate the stone into “dust-like" fragments that can spontaneously pass; or *fragmentation with extraction* in which lower frequency pulses are delivered to break the stone into larger fragments for subsequent removal with an auxiliary stone basket [4].

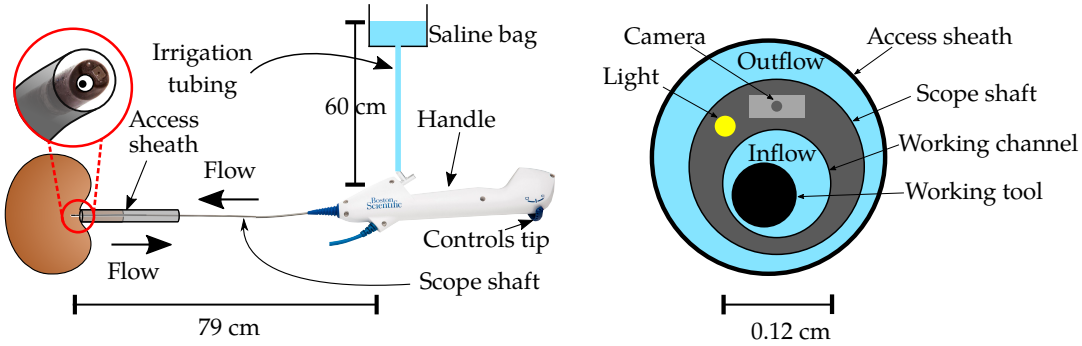

Figure 1 – A photograph of a Boston Scientific ureteroscope (left) with the tip of the scope circled and a zoomed-in schematic provided of the scope tip (right). The scope lies within an access sheath, and a working tool sits inside the working channel. A camera and a light are embedded in the scope wall. Dimensions of the scope shaft and working channel are labelled.

Resulting particles and debris obstructing the field-of-view for the operating surgeon is an undesirable outcome of stone lasering. To mitigate this, a saline bag is hung above the patient and connected to the working channel via vertical tubing. This provides *irrigation*, a continuous fluid flow through the *irrigation tubing*, the working channel, out of the scope tip, and into the renal pelvis. The fluid exits the body in the opposite direction, along the outside of the scope shaft. There is only a narrow gap between the scope and the ureteral wall, and if too much saline is delivered, overfilling of the kidney (and hence elevated renal pressures) may occur. High kidney pressures during ureteroscopy have been linked to infective post-operative complications, such as sepsis [5]. Thus, to prevent kidney pressures from rising unduly, many urologists insert the scope through a ureteral access sheath; a hollow cylinder that surrounds the scope, temporarily widening the ureter to allow irrigation fluid to flow more freely back out of the kidney alongside the shaft of the scope (Figure 1). The use of ureteral access sheaths has been shown to decrease the risk of postoperative complications, with no effect on stone-removal success [6].

Our challenge

Optimising the flow of irrigation fluid through the ureteroscope to maintain good visualisation during surgery is a universal urological challenge. Ideally, irrigation flow would aid visualisation without causing detrimentally high intrarenal pressures. Determining the optimal flow requires a good understanding of the fluid mechanics of ureteroscopes, and how the irrigation system behaves under operating room conditions. We combine mathematical modelling and physical experiments to build a mechanistic understanding of the fluid mechanics of ureteroscopy irrigation.

Glossary of terms

- **Volumetric flow rate:** The volume of fluid that flows, per unit time.
- **Hydrostatic pressure head:** Pressure exerted by a stationary column of fluid – depends only on the height, gravity, and the denisty of the fluid.
- **Elliptical eccentricity:** A measure of how non-circular an ellipse is – $e = 0$ is a circle and $e = 1$ a slit of zero width and infinite length.
- **Advection:** The transfer of matter by the flow of fluid.
- **Diffusion:** The movement of matter from high concentration to low concentration.

2 Flow through an isolated scope

We first model the flow of irrigation through the ureteroscope outside the urinary system, considering the influences of saline bag height, deflection of the scope, and the presence of the working tools. The equations, derived through conservation of mass and a balance of forces, relate the volumetric flow rate of irrigation fluid to properties of the scope and the geometry of the irrigation setup. To test our model predictions we also conduct experiments in a controlled laboratory configuration.

Saline bag height

The volumetric flow rate Q of irrigation fluid through the ureteroscope is dependent on the inlet pressure P_{in}, the working channel radius a, the scope length L, and the density and dynamic viscosity of the irrigation fluid ρ and μ, respectively. Assuming the flow remains laminar, the relation is:

$$Q = \frac{a^4 \pi P_{\text{in}}}{8\mu L} \tag{1}$$

If the column of irrigation fluid within the tubing connecting the saline bag to the scope creates a hydrostatic pressure head we expect $P_{\text{in}} = \rho g H$, where H is the vertical distance from the scope inlet to the surface of irrigation fluid within the saline bag. Equation (1) is plotted with hydrostatic inlet pressure as the dashed black line in Figure 2a anticipating a linear relationship between H and Q. We observe a systematic deviation between this linear prediction and experiment, which becomes more pronounced at higher head heights. We propose that the deviation mostly arises from neglecting the viscous dissipation due to the vertical flow that occurs from the suspended reservoir into the scope. Accounting for fluid flowing through the irrigation tubing, the adjusted inlet pressure is predicted to be:

Volumetric flow rate increases non-linearly with saline bag height.

$$P_{\text{in}} = \rho g H \left(1 - \frac{\sigma}{1+\sigma}\right) \tag{2}$$

where $\sigma = (H/L)(a/\ell)^4$ with ℓ the radius of the irrigation tubing. Equation (2) characterises the relative importance of viscous dissipation through the vertical tubing. As H increases (or ℓ decreases), σ will increase and the imposed pressure difference is increasingly smaller than $\rho g H$. In Figure 2a, the model prediction with P_{in} specified by equation (2) is shown as the solid line, which indeed shows superior agreement with the experiment.

For the parameters explored here, viscous dissipation becomes increasingly significant as the height of the irrigation fluid increases (Figure 2a). We thus conclude that even in

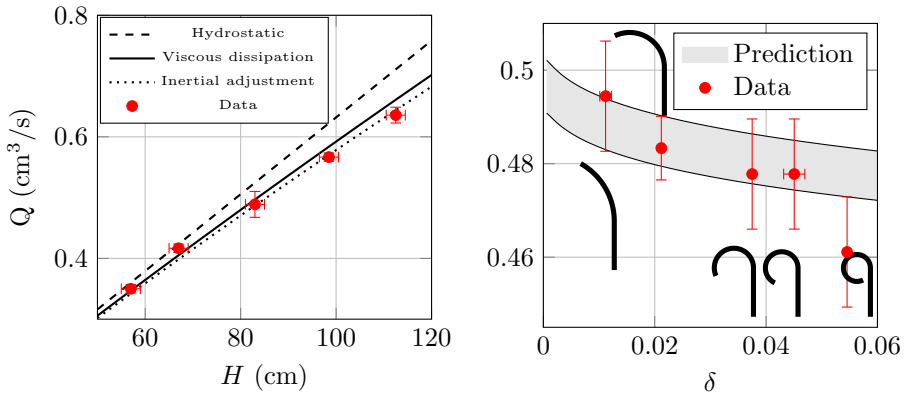

(a) Effect of saline bag height. **(b) Effect of tip deflection.**

Figure 2 – Experimental (red data points) and theoretical results (black lines) for the flow of water through an open ureteroscope working channel of internal radius 0.06 cm. (a) Dashed line assumes a hydrostatic inlet pressure and solid line accounts for viscous dissipation through the irrigation tubing. (b) The solid black lines surrounding the gray predictive region provide predictions for the minimal and maximal height (accounting for experimental error). Height is set at $H = 83$ cm.

this simple setting, classic results may yield inaccurate predictions. In a clinical setting, the dependence of the volumetric flow rate on both height and tube radius should be considered when determining how high to hang the irrigation bag.

Ureteroscopic pipe fittings

We notice there is still a small discrepancy between the solid black line and the red data points in Figure 2a. We hypothesise that this occurs due to a pressure loss as fluid flow changes from the vertical irrigation tubing of radius 0.125 cm to the horizontal working channel of radius 0.06 cm. As the velocity patterns corresponding to flow through the connection between the irrigation tubing and the working channel are undoubtedly complicated, a unifying governing theory is unattainable. However, an ability to capture changes in pressure resulting from pipe contractions, expansions, bends, entrances, and exits is an invaluable tool to estimate flow through hydraulic networks of particular configurations. To this end, constitutive laws have been constructed from empirical measurements, and common practice is to encapsulate the behaviour of the flow and associated dissipated kinetic energy for each sudden change in pipe geometry with a single dimensionless parameter, K. For example, to estimate the inlet pressure in Figure 2a:

$$P_{\text{in}} = \rho g H - \frac{8\mu H}{\pi \ell^4} Q - \frac{K\rho}{2(\pi \ell^2)^2} Q^2 \tag{3}$$

If $K = 0$ equation (3) reduced to equation (2). With K as a fitting parameter, we obtain the line in Figure 2a with best-fit value $K \approx 1.77$.

A valuable tool for the urological community would be a look-up table relating saline bag height to flow rate. However, due to bespoke fittings between components of the irrigation system, there will inherently be a degree of uncertainty in estimating volumetric flow rates from system parameters. One possibility to mitigate this ambiguity is through the use of gradual geometric changes (e.g. between the irrigation tubing and the working channel) rather than abrupt contractions [7]. This allows streamlines to adhere to the changing geometry, avoiding fluid detachment and recirculation that is induced with abrupt geometric adjustments. Appropriately accounting for pressure losses due to each component of a ureteroscopy irrigation system is imperative. If large reductions in flow rate from fully-developed predictions are observed, design alterations to lessen the flow disruptions caused by connectors and fittings may be initiated.

The geometric contraction and bend from irrigation tubing to working channel causes a reduction in flow rate.

Scope deflection

Scope deflection causes a small decrease in flow rate.

We now consider the effect of ureteroscope deflection on the volumetric flow rate. A 6 cm length at the distal end of the scope can curve while the majority of the scope remains straight. We adapt the previous flow model to describe flow through a scope with a deflected tip; this involves considering flow through a pipe with constant curvature. From curved pipe theory, we deduce that flow rate is dependent upon the Dean number, a dimensionless parameter that relates centripetal, inertial, and viscous forces, and that different flow rate relations can be implemented depending upon the magnitude of this value. From these results, we conclude that the flow through a curved scope depends upon the curvature of the tip $\delta = a/R$, where R is the radius of curvature, along with the previous relevant parameters. In Figure 2b, we plot the volumetric flow rate as a function of curvature. The two solid black lines in Figure 2b show the minimal and maximal theoretical predictions, with regards to the error in measuring the inlet pressure. Our model also predicts that the flow rate will decrease linearly with the arc length of the curved portion of the scope, although this result is not shown. However, in any case, the decreases in volumetric flow rate are all relatively minimal, e.g., the highest curvature possible for Boston Scientific's LithoVue™ ureteroscope corresponds to only a 5% decrease in flow rate from that of a straight scope.

Working tools

Flow rate decreases with working tool size.

We next consider the effect of inserting working tools through the scope on irrigation flow. In Figure 3a, we plot the results of experiments measuring the flow rate through a ureteroscope with various Boston Scientific working tools (Table 1), compared with the predictions of our mathematical model. We see that the presence of a working tool reduces the cross-sectional area available for fluid and thus reduces the flow. The degree of reduction increases with the radius of the working tool; a larger tool hinders irrigation flow more.

	Working tool	Radius ($\times 10^{-2}$ cm)
(a)	No tool	
(b)	OptiFlex™ basket	2.17
(c)	Flexiva™ 200 Laser Fibre	2.21
(d)	Flexiva™ 365 Laser Fibre	3.02
(e)	Zero Tip™ basket	3.17
(f)	ZIPwire™	4.83

Table 1 – Working tools corresponding to the data points in Figure 3a.

An elliptical working channel allows higher flow than a circular channel of equal area.

In practice, the position of the tool within the working channel is unknown, and the predictions show that flow through the working channel containing a working tool increases with tool proximity to the channel edge. This is shown in Figure 3a; the lower black line is the prediction for a concentric tool, and the upper black line for a fully offset tool, with the grey region between indicating flow predictions for all possible positions of the working tool. The thickness of the grey region in Figure 3a demonstrates the basic physical principal that flow resistance created by the presence of a working tool is strongly tied to the geometry of the space available for fluid flow. This motivates the question of whether a more optimal channel configuration could be realised with a non-circular cross-section for the working channel. We consider an elliptically shaped cross-section of fixed cross-sectional area. In Figure 3b we consider the dimensions of the Flexiva™ 365 Laser Fibre (data point (d) in Figure 3a) and plot flow rate as a function of the elliptical eccentricity of the working channel, when the tool is placed at the position that maximises flow rate. The maximum flux over all eccentricity values for the outer ellipse (data point (*ii*)) is nearly 50% higher than the flux for a circular outer cylinder of the same cross-sectional area (data point (*i*)).

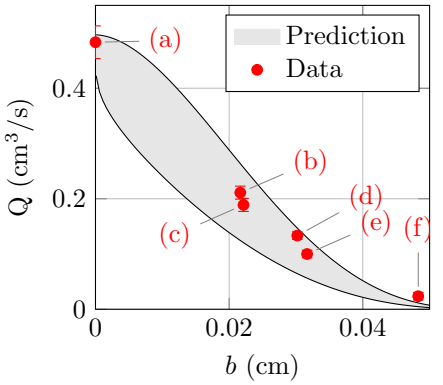

(a) Effect of working tools.

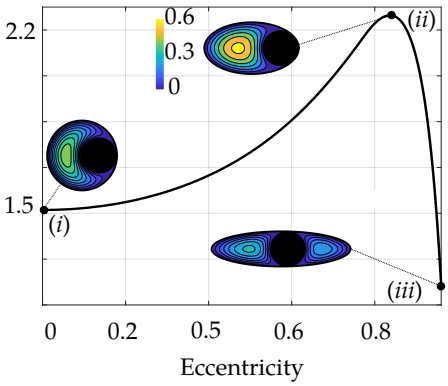

(b) Elliptically shaped working channel containing Flexiva ™ 365 Laser Fibre.

Figure 3 – (a) Experimental and theoretical results for flow through a working channel containing a working tool with the column of irrigation fluid at height $h = 83$ cm. The grey region indicates flow predictions for a circular working channel; the lower line for a tool concentric within the working channel and the upper line for a tool at the edge. The tools used are listed in Table 1.

3 Flow through the full irrigation system

Models for flow in through the working channel and out through the access sheath are combined by considering a conservation of irrigation flux and modelling the kidney as an elastic body containing irrigation fluid at constant pressure. We assume that the volume of the kidney and the intrarenal pressure are related by a constitutive exponential law, motivated through a fit to experimental data [9]. We subsequently obtain an expression for kidney pressure which increases with inlet pressure and is affected by resistance to flow through the working channel and access sheath. We consider the effect of working tools by increasing flow resistance through the working channel (using the model validated in the previous section); this results in decreased kidney pressure and flow rate for fixed inlet pressure. Decreasing flow resistance through the access sheath by modifying the cross-section geometry (see Figure 3b) results in decreased kidney pressure but increased flow rate, both desirable attributes of ureteroscopy.

4 Clearance of kidney stone dust

We model irrigation flow within the renal pelvis by considering the reduced, two-dimensional geometry in a Cartesian coordinate system pictured in Figure 4. The

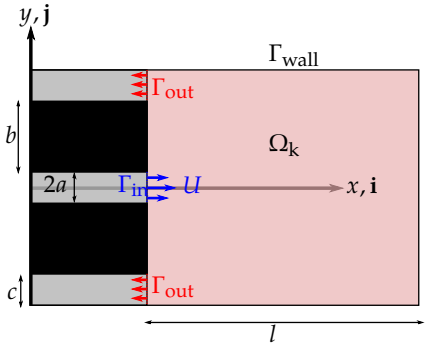

Figure 4 – The idealised geometry. The light pink rectangle denotes the domain, Ω_k. The black rectangles represent the solid scope shaft, with grey regions indicating inflow through the working channel and outflow through the sheath alongside the scope shaft. The labelled lengths indicate: cavity length l, working channel half-width a, scope shaft half-width $a + b$, and cavity width $a + b + c$.

black rectangles symbolise the solid scope shaft, with grey areas denoting fluid-filled

inflow and outflow channels. The light-pink region in Figure 4 denotes the renal pelvis domain Ω_k with inflow and outflow boundaries Γ_{in} and Γ_{out}. We assume fixed values for a, b, and c motivated by typical working channel, scope shaft, and access sheath dimensions in ureteroscopy. Therefore, we focus on quantifying the flow structure as a function of three important parameters: the flow rate, the scope position (centred or offset), and the length l, of the cavity (see Figure 4). In a ureteroscopy context, these parameters could be varied by the operating staff by changing the height of the irrigation bag, or by adjusting the distance between the scope tip and proximal kidney walls, respectively. We numerically solve the steady Navier-Stokes equations, which are derived from a conservation of mass and a balance of forces, within Ω_k (Figure 4). Numerical and experimental (particle image velocimetry) results are in excellent agreement and are provided in Chapter 5 of [10]. The flow is characterised by a variety of vortical structures, see Figure 5.

To determine the effect of flow structure on the time required to clear the renal pelvis of stone particles and debris, we solve an advection diffusion equation for the concentration of a cloud of tracer that diffuses and is passively advected by the flow. The competing effects of advection and diffusion are characterised by a dimensionless parameter, the Peclet number Pe – increasing Pe decreases the relative effect of diffusion with respect to advection. We find, that if a circular tracer cloud initiates in a region of closed streamlines (a vortex) the time required for 90% of the tracer to exit the renal pelvis – termed T_{90} – is large, particularly if diffusion is weak with respect to advection. Results are summarised in Figure 5 where A, B, C, D, and E correspond to five different starting positions within a representative flow pattern. Colours correspond to dimensionless washout time T_{90} shown in the colourbar in Figure 5. In [10] we discuss a flow manipulation strategy to remove the passive tracer from vortices by instantaneously changing the flow pattern.

Stone dust trapped in vortices takes a prolonged time to clear.

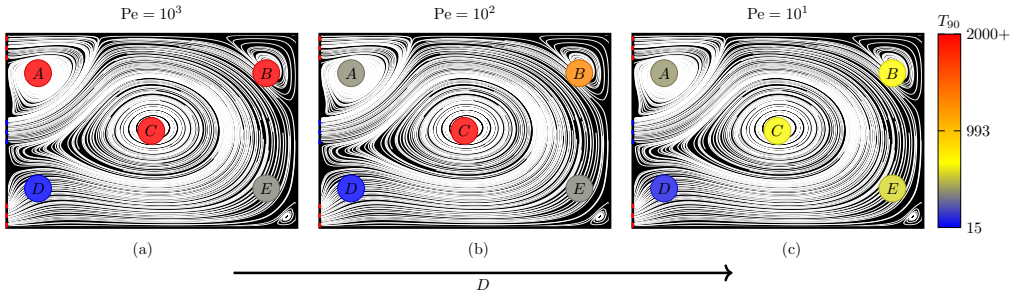

Figure 5 – Washout time for five different dust starting positions. Figures (a), (b), and (c) are for Pe = 10^3, 10^2, and Pe = 10^1.

5 Discussion, conclusions, & recommendations

We have presented experimental and theoretical results on the irrigation flow during ureteroscopy. We first considered an isolated ureteroscope and determined the effects of saline bag height, tip deflection, and working tools. Flow rate increased non-linearly with bag height due to viscous dissipation through the irrigation tubing; flow rate decreased negligibly with tip deflection; flow rate decreased with the addition of working tools. Care must be taken when bolting together classic linear relationships between flow rate and pressure drop as ureteroscopic pipe fittings contribute non-linear effects. Flow rate through an isolated scope containing a working tool is increased by moving the tool from the centre to the edge of the working channel and by modifying the cross-sectional shape of the working channel from circular to elliptical. We obtained simple formulas for kidney pressure and flow rate as functions of system parameters by equating inflow through the working channel with outflow through the access sheath, considering the kidney to be exponentially compliant. Importantly, flow rate increased and kidney pressure decreased with decreasing outflow resistance, which motivated consideration of an elliptical access sheath geometry. Finally, we turned to modelling flow within a simplified geometry representing the renal pelvis. The flow was found to contain multiple vortices, and placing a passive tracer initially within these vortices incurred large times to wash the tracer from the cavity.

6 Potential impact

The flow of irrigation through ureteroscopes has been examined in previous experimental studies, but we are the first to apply a mathematical modelling approach to this system. Our work serves as preliminary modelling steps towards developing a generic framework for describing flow in ureteroscopes. Such a tool, adaptable to different physiological conditions and scope parameters, would have immense potential value, both in advising scope design and as an optimization guide for physicians in scope procedures.

Tim Harrah, a manager at Boston Scientific, commented: *After a decade of market leadership making tools used through endoscopes, Boston Scientific has recently entered the market as a producer of visualization systems. For surgeries done using an endoscope, good visualization is synonymous with good fluid management. Unfortunately the literature for fluid delivery in endoscopic surgery is sparse. Work on this project has already contributed meaningfully to our understanding and we are excited to extend the underlying modeling framework to address other opportunities to make endoscopic surgeries more efficient and effective.*

References

[1] K.K. Stamatelou, M.E. Francis, C.A. Jones, L.M. Nyberg, and G.C. Curhan. Time trends in reported prevalence of kidney stones in the United States: 1976-1994. *Kidney International*, 63(5): 1817–1823, 2003. ISSN 00852538. doi: 10.1046/j.1523-1755.2003.00917.x.

[2] C.D. Scales, A.C. Smith, J.M. Hanley, and C.S. Saigal. Prevalence of kidney stones in the United States. *European Urology*, 62(1):160–165, 2012. ISSN 03022838. doi: 10.1016/j.eururo.2012.03.052.

[3] J.B. Basillote, D.I. Lee, L. Eichel, and R.V. Clayman. Ureteroscopes: Flexible, rigid, and semirigid. *Urologic Clinics of North America*, 31(1):21–32, 2004. ISSN 00940143. doi: 10.1016/S0094-0143(03)00094-6.

[4] B.R. Matlaga, B. Chew, B. Eisner, M. Humphreys, B. Knudsen, A. Krambeck, D. Lange, M. Lipkin, N.L. Miller, M. Monga, V. Pais, R.L. Sur, and O. Shah. Ureteroscopic Laser Lithotripsy: A Review of Dusting vs Fragmentation with Extraction. *Journal of Endourology*, 32(1):1–6, 2018. ISSN 1557900X. doi: 10.1089/end.2017.0641.

[5] W. T. Wilson and G. M. Preminger. Intrarenal pressures generated during flexible deflectable ureterorenoscopy. *J. Endourol.*, 4(2):135–141, 1990. ISSN 1557900X. doi: 10.1089/end.1990.4.135.

[6] O. Traxer, G. Wendt-Nordahl, H. Sodha, J. Rassweiler, S. Meretyk, A. Tefekli, F. Coz, and J.J. de la Rosette. Differences in renal stone treatment and outcomes for patients treated either with or without the support of a ureteral access sheath: The Clinical Research Office of the Endourological Society Ureteroscopy Global Study. *World Journal of Urology*, 33(12):2137–2144, 2015. ISSN 14338726. doi: 10.1007/s00345-015-1582-8.

[7] F.M. White. *Fluid Mechanics*. McGraw-Hill, New York, 7 edition, 2008.

[8] J.G. Williams, B.W. Turney, D.E. Moulton, and S.L. Waters. The effect of elliptical geometries on resistance in annular pipe flows. *Journal of Fluid Mechanics*, (Submitted):1–44, 2019.

[9] J.G. Williams, S.L. Waters, D.E. Moulton, L. Rouse, and B.W. Turney. A lumped parameter model for kidney pressure during stone removal. *IMA Journal of Applied Mathematics*, Submitted, 2019.

[10] J.G. Williams. *Mathematical modelling of ureteroscopic flows during kidney stone removal*. PhD thesis, University of Oxford, 2019.